

PHOENIXOS: Concurrent OS-level GPU Checkpoint and Restore with Validated Speculation

Xingda Wei^{†1}, Zhuobin Huang^{†2}, and Tianle Sun, Yingyi Hao, Rong Chen, Mingcong Han, Jinyu Gu, Haibo Chen¹

¹Institute of Parallel and Distributed Systems, Shanghai Jiao Tong University

²National University of Singapore

Abstract

PHOENIXOS (PHOS) is the first OS service that can concurrently checkpoint and restore (C/R) GPU processes—a fundamental capability for critical tasks such as fault tolerance, process migration, and fast startup. While concurrent C/R is well-established on CPUs, it poses unique challenges on GPUs due to their lack of essential features for efficiently tracing concurrent memory reads and writes, such as specific hardware capabilities (e.g., dirty bits) and OS-mediated data paths (e.g., copy-on-write).

To ensure correct concurrent C/R, PHOS proactively detects GPU memory reads and writes through a two-step process: first, it speculates about GPU memory accesses based on the arguments used when launching GPU kernels; then, it validates these accesses efficiently at runtime using binary instrumentation. With this validated speculation, PHOS retrofits CPU-based concurrent C/R for GPUs through software-based approaches, including soft copy-on-write, soft recopy, and soft on-demand restore. PHOS further proposes several GPU-aware techniques for efficient GPU C/R, including coordinated checkpoint data transfer and execution context pool. For downstream tasks that use C/R for tolerating failures, migrating processes live, and accelerating cold starts in serverless computing, PHOS achieves orders of magnitude higher performance than state-of-the-art OS-level GPU C/R systems like NVIDIA cuda-checkpoint.

1 Introduction

What is and why concurrent OS-level checkpoint and restore (C/R). OS-level checkpoint snapshots the execution of a running process as an image, which the OS can then use to restore the execution of the process. It is a foundational OS primitive: cluster management systems rely on it to migrate tenant jobs [63, 74, 55], by first checkpointing the image to the target machine, then restoring from it. Serverless systems leverage OS-level restore to quickly start new processes [15, 32, 20]. Cloud providers periodically checkpoint computing jobs to provide fault tolerance for them [63, 73].

A key feature of OS-level checkpoint and restore is its

transparency to the process, making it irreplaceable for functionality and efficiency in various scenarios. For functionality, consider cloud providers that need to migrate tenant jobs to improve cluster utilization and for other purposes [63, 74, 55]. Since these jobs operate as black boxes to the provider [55], migration can only be performed at the OS level. For efficiency, consider serverless platforms that need to quickly start GPU processes [16]. These processes have PyTorch runtime states (e.g., compiler cache) that are tightly intertwined with OS information. Recreating these states from scratch takes seconds; thankfully, OS-level C/R can significantly reduce this overhead by first checkpointing the process state and then restoring it within 10 milliseconds [20, 72, 67].

Additionally, OS-level C/R can also provide superior usability [63, 45], which is why major cloud providers (e.g., Microsoft Forge [45, 28]) employ it for fault tolerance. The key rationale is that performing efficient and correct fault tolerance through user-level checkpointing is challenging due to the broad optimization space and quickly evolving workloads [71, 46, 68]. For instance, Megatron [50], the leading LLM training framework, has recently integrated concurrent checkpoint optimizations proposed three years ago [46], with the checkpoint code now comprising a quarter of its codebase. Meanwhile, many emerging training frameworks, such as those for reinforcement learning [57], still lack these optimizations. With efficient OS-level checkpointing, applications can avoid the burden of implementing and optimizing their own fault tolerance mechanisms.

Concurrent OS-level C/R—performing checkpoint and restore while allowing processes to run concurrently—is becoming increasingly important, as stopping GPU processes severely impacts application performance due to the lengthy data copy time during the C/R process (§2.3). For example, Microsoft reports that over 3.9% of GPU users experience quality issues from process migration stalls using C/R [26]. The stall caused by restoring a Llama-2-13B inference using state-of-the-art OS-level C/R [63] requires a 6.2-seconds pause—31× longer than the Time-To-First-Token (TTFT) for inference, which significantly hinders deploying GPU processes in emerging serverless computing [33, 16]. Finally, in fault tolerance scenarios like model training, the checkpoint time can be comparable to the iteration time (46–87%, see §8), and hiding them with concurrent execution can save precious

[†]Xingda Wei and Zhuobin Huang contributed equally. Part of the work was done when Zhuobin Huang was an intern at Institute of Parallel and Distributed Systems, Shanghai Jiao Tong University.

Table 1: An overview of the information (Info.) required for correct concurrent checkpoint and restore, and how PHOS tracks them.

	Info.	CPU	GPU
Checkpoint	Writeset	Permission [73, 66] and dirty bits [14]	Speculation + Validation
Restore	Readset	Present bits [72, 20, 69]	(§4.1)

GPU hours [71, 68, 46, 31].

Current systems and the key challenge. Existing systems like NVIDIA’s cuda-checkpoint [63, 56] cannot perform concurrent checkpoint and restore of GPU-related states. While concurrent execution of C/R is standard practice for CPU processes, it is ineffective when the GPU is stopped because the CPU must wait for GPU execution results (§2.3). This raises a key question: *Can we achieve efficient and effective OS-level checkpoint and restore during concurrent GPU execution?*

The key challenge is ensuring correctness—a checkpoint must reflect a valid process state as if no checkpoint had occurred (§4). For example, if the GPU executes two kernels before the checkpoint, the checkpoint must capture the exact state of GPU memory after these two kernels write. However, the process running concurrently can overwrite data that has not been checkpointed, resulting in an incorrect checkpoint. Similarly, during the restore, if a GPU kernel reads data while the OS is concurrently restoring it, the kernel may read incorrect data, corrupting the process state.

The key for correctness is to trace the read and write sets of the concurrent execution, i.e., which bytes of CPU/GPU states are read and written by the process. Take checkpointing as an example: the OS can use this information to isolate the writes that cause an incorrect checkpoint with copy-on-write [61, 73], or recopy the writes to the checkpoint [14] for correctness. For CPU states, the OS can leverage OS-mediated data paths with hardware paging to gather this information, as summarized in Table 1. However, GPUs lack the necessary hardware support [27] and bypass the OS during their execution to maximize performance.

Key insights. Unlike CPU, whose execution is a coarse-grained black box to the OS, the execution of GPU is composed of fine-grained units (e.g., kernels), whose control flow is mediated by the OS. Specifically, applications trigger GPU execution through fine-grained GPU API calls (e.g., CUDA [49]), which the OS can intercept to trace their read and write sets for concurrent checkpoint and restore. Because each API will trigger fine-grained GPU state modifications (§8.4), such an API-level tracing can realize an efficient and correct concurrent C/R.

However, tracing read and write sets at the API level is non-trivial, because although some APIs have well-defined read and write semantics, e.g., those launch kernels provided by the vendors like cuBLAS [52], the process can also trigger user-developed kernels that may contain arbitrary code. Fortunately, we find that although such kernels may include

complex code, each typically serves a clear and straightforward computational purpose, such as matrix multiplication or convolution operations. This makes it possible to accurately speculate which data will be accessed by simply analyzing the kernel’s launch arguments (§4.1).

The PHOENIXOS (PHOS). Based on our insights, we built PHOS, the first OS service capable of concurrently checkpointing and restoring GPU processes. PHOS speculates the data accessed by each GPU execution unit using its launch arguments, and uses this speculated information to retrofit CPU-based concurrent C/R protocols for GPUs, including soft copy-on-write (§4.2), soft recopy (§4.3), and soft on-demand restore (§6). To ensure correctness, we further instrument a lightweight validator to correctly handle speculation failures.

Retrofitting CPU-based concurrent C/R techniques on GPUs with our validated speculation—although ensures correctness—still suffers from performance issues if not considering the features of GPUs carefully. First, during concurrent checkpoint, the interference between CPU and GPU checkpoint, as well as between application data transfers and checkpoint transfers, can significantly impact the efficiency and effectiveness of the concurrent checkpoint. To mitigate these interferences, we design a coordinated and prioritized checkpoint mechanism (§5). Second, before allowing a concurrent restore, we must create the proper GPU execution environment, which incurs overhead comparable to that of data restoration itself. We propose using a GPU context pool to bypass the context creation and fully unleash the power of concurrent restore (§6).

Demonstrations. PHOS runs on Linux and it can C/R unmodified GPU applications (including multi-GPU processes) on NVIDIA GPUs. We chose NVIDIA GPUs due to their prevalent adoption, despite higher implementation complexity. Nevertheless, our design also generalizes to other GPUs and accelerators, because they follow the same execution model PHOS assumed for NVIDIA GPUs (§2.1). On A800 GPU servers, when compared to state-of-the-art systems—Singularity [63] and NVIDIA’s official OS-level C/R (cuda-checkpoint) [56], PHOS reduces the application stall caused by checkpoint and restore by up to 160%. More importantly, PHOS brings orders of magnitude improvements on end-to-end application performance across various tasks. Notably, compared to Singularity, it reduces the wasted GPU time by 76% when training Llama3-13B on multiple GPUs, it reduces the downtime caused by migrating a Llama2-13B inference job from 9.8 to 2.3 seconds, and it can cold-start a Llama2-13B inference job within only 622 milliseconds, which is 124–450% and 114–342% faster than cuda-checkpoint and Singularity, respectively.

Contributions. We highlight our contributions as:

- The first efficient GPU execution read and write set detection via validated speculation (§4.1).

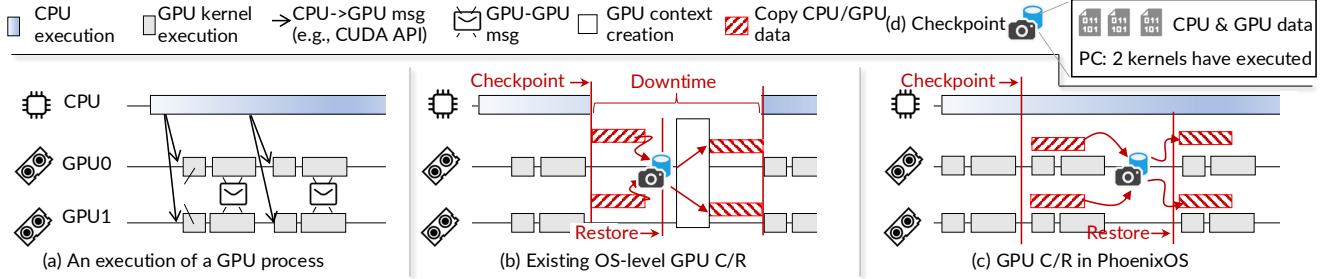


Figure 1: Illustrations of (a) how a GPU process executes, (b) how a stop-the-world OS-level checkpoint and restore works, (c) how PHOS does checkpoint and restore, and (d) the main content of checkpointed data.

- The first set of OS-level concurrent checkpoint and restore protocols for GPUs (§4.2, §4.3, and §6) that ensure correctness with validated speculation.
- PHOS is the first OS-level concurrent checkpoint and restore system for GPUs. It addresses several technical challenges to realize the concurrent protocols (§5 and §6), and it significantly enhances various end-to-end application performance (§8).

PHOS will be open-sourced upon publication.

2 Background and Motivation

2.1 How a process uses GPUs

GPUs are accelerators with massive multithreading typically attached to the CPU via PCIe. Programs executed on GPUs are termed *kernels*, which contain machine code (e.g., SASS [54]) that is either pre-compiled or just-in-time compiled. Kernels process data residing in GPU *buffers*, where each buffer constitutes a contiguous GPU virtual memory region with application-controlled granularity.

When a process starts, the GPU driver creates proper execution context, e.g., CUcontext [53], involving loading or compiling the kernel binaries and configuring the GPU virtual memory [42]. Afterward, processes use standardized GPU driver or toolkit APIs (we term *GPU API* in this paper) like CUDA [49], illustrated in Figure 1 (a), to trigger computations on GPUs. For example, the process can launch kernels via `cudaLaunchKernel` and copy CPU data to GPU using `cudaMemcpy`. Due to the limited control capability of GPUs, the GPU execution is orchestrated by the CPU by calling GPU APIs based on the application’s logic. PHOS intercepts GPU APIs for realizing checkpointing and restoration, thus supporting all GPU applications at the OS-level.

2.2 OS-level GPU checkpoint and restore (C/R)

Basic checkpoint and restore. A checkpoint captures a process’s execution state at a specific time in an image (termed as *checkpoint*). The OS can then use this checkpoint to recreate (restore) the process. A checkpoint includes two data categories: data state (data in the CPU virtual memory and GPU

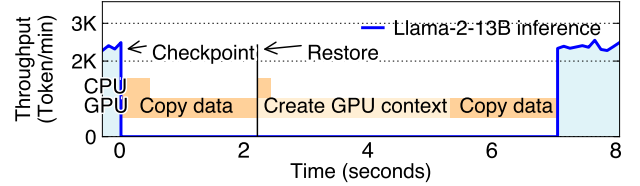


Figure 2: A breakdown of checkpoint and restore overhead.

buffers) and control state (e.g., CPU registers that store the program counter, PC). The checkpointed CPU states also include kernel objects like network connections [17, 66].

A common approach for implementing GPU checkpointing is by quiescing process execution (both CPU and GPU), i.e., stops the CPU execution and waiting for all in-flight GPU kernels and communications to finish, then copying all aforementioned data to the checkpoint [56, 63]. Figure 1 (b) illustrates this. For restoration, the OS first loads data state into CPU memory and GPU buffers, then restores control state to resume execution.

Concurrent CPU checkpoint and restore. To prevent application stall during checkpointing and restoration, which has non-trivial overhead, OS researchers have investigated concurrent CPU checkpointing and restoration for decades [73, 66, 14, 72, 20, 69]. Concurrent checkpointing allows CPU execution during data copying, thus hiding the overhead of checkpointing. For correctness, the OS either isolates concurrent CPU writes via copy-on-write [73, 66], or recopies concurrently written data to the checkpoint [14]. Concurrent restoration enables immediate process resumption, i.e., no need to wait for the restoration to finish. During the process execution, the data is being concurrently copied from the checkpoint to the CPU memory. For correctness, if the process touches non-restored data during execution, the CPU will trigger a page fault, so the OS will copy the missing data from the checkpoint on demand [72, 20, 69].

2.3 Key factors stalling applications during C/R

Figure 2 analyzes the stalls caused by checkpoint and restore on a Llama2-13B inference process. We evaluate Singularity [63]—the state-of-the-art GPU checkpoint and restore system, other baselines like cuda-checkpoint [56] are much slower. We have enabled concurrent CPU checkpointing and

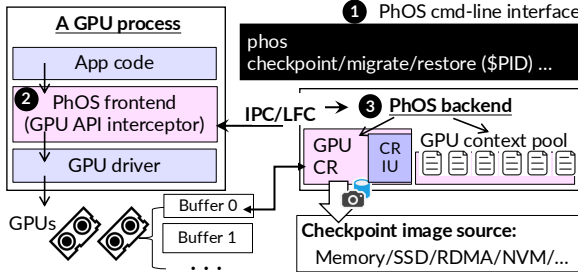


Figure 3: PHOS system architecture. Note that IPC and LFC stand for inter-process call and local function call, respectively.

restoration using CRIU’s incremental dump and restore [19]. The detailed setup and performance of cuda-checkpoint can be found in §8.

Copying GPU data. Because the GPU is stopped when copying data to and from checkpoint, the applications are stalled despite the CPU-side of the process being concurrently executed. The stall time is non-trivial: checkpointing and restoring data each require more than 2.1 seconds respectively when transferred with PCIe, causing thousands of tokens to be disrupted. The stall further scales with the GPU memory used, which is substantial: For instance, Llama2-13B inference occupies 56 GB of active memory. Given a typical 32 GBps PCIe 4.0 CPU-GPU link, OS-level checkpoint and restore takes at least 1.75 seconds.

Creating GPU contexts. Before restore can copy data to the GPU, the OS must create proper GPU contexts. This establishes a restoration barrier as context creation incurs comparable overheads to data copying, i.e., 3.1 vs. 1.7 seconds in our motivation experiment. GPU context initialization exceeds CPU context creation time due to complex hardware configuration and driver state loading [42]. In comparison, creating CPU context, i.e., a Linux process, merely initializes a small number of kernel data structures.

3 The PHOS Operating System

Design goals. Our goals are *efficient* and *correct* OS-level GPU checkpoint and restore. For efficiency, the goal is to minimize process stalls during checkpoint or restore. PHOS achieves this through: concurrent process execution during data copying for both checkpoint and restore, and bypassing GPU context creation during restore, as illustrated in Figure 1 (c). For correctness, the goal is to make the checkpoint reflect an application state indistinguishable from a non-checkpointed execution [63, 37, 66].

System architecture and execution flow. Figure 3 shows PHOS’s architecture that has three core system components: a command-line tool (1), a per-process frontend library to facilitate C/R (2), and a backend module to do the C/R (3).

Our command-line tool (1) enables users to checkpoint running GPU processes, migrate them across machines, or re-

store processes from checkpoints with the process ID (\$PID). Though PHOS does not require application cooperation, we found that it can benefit from choosing a proper checkpoint time (see §8.3), so we also provide an SDK for applications to control the timing with only six lines of additional code (Details are left in §A.2 due to space limitation).

Once a checkpoint or restore command is received by the tool, it will communicate with the frontend library (2) embedded in the GPU driver and its toolkits. The frontend will call our backend to do the checkpoint and restore, as well as trace the read and write sets (§4.1) when the process calls a GPU API. This information is provided to our C/R backend to ensure correctness (§4 and §6). Our current implementation leverages `LD_PRELOAD` to extend the CUDA GPU API as CUDA is closed-source, but `LD_PRELOAD` is not a requirement once the code is available.

Our backend (3) uses CRIU [18] to checkpoint and restore CPU process states, and our efficient GPU engine (see §5) for GPU states. Choosing CRIU allows PHOS to correctly checkpoint and restore complex states like network connections. We support a wide range of checkpoint media: PHOS can read and write checkpoints to local SSD, CPU DRAM and even the DRAM of another machine via RDMA (§7), which is critical for efficient process migration. The backend also includes a GPU context pool—containing pre-allocated contexts that avoid creating GPU contexts during restore (§6).

PHOS command-line tool uses inter-process calls (IPC) to communicate with the frontend. On the other hand, the frontend and backend can communicate either via IPC or local function calls (LFC). We prefer LFC when feasible by linking the frontend and backend in the same library. However, our context pool requires storing the pool in an OS service daemon, so LFC is not possible. Thus, for scenarios that require the context pool, e.g., serverless startup [33, 16], we use IPC. For others like fault tolerance we employ LFC. The IPC overhead remains minimal because GPU APIs execute asynchronously, allowing overlapping IPC cost with GPU execution [70, 76].

4 Making concurrent GPU checkpoint correct

Correctness guarantee of PHOS. Intuitively, a checkpoint is correct if it could occur in a checkpoint-free execution [23]. A stop-the-world checkpoint described in §2.2 naturally guarantees correctness. PHOS ensures correctness by ensuring that our checkpoint matches the one that may come from the existing stop-the-world checkpoint.

Overview of the checkpoint protocols. We retrofit two CPU-inspired protocols [73, 66, 14]. As Figure 4 shows, consider our checkpoint starting at t_1 with concurrent data copy done at t_2 . Compared with a stop checkpoint at t_1 , inconsistencies are caused by new writes issued between $[t_1, t_2]$. Our soft copy-on-write (CoW) protocol isolates these writes (§4.2), making the checkpoint only copy a frozen GPU state

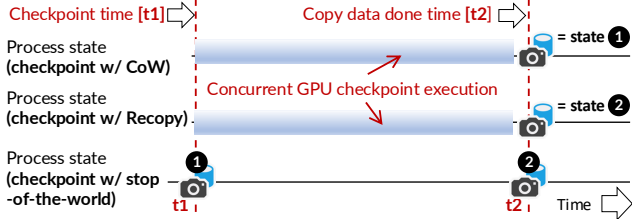


Figure 4: An illustration of correctness guarantee of concurrent checkpointing enabled by different protocols of PHOS.

at t_1 . Alternatively, compared to a stop checkpoint at t_2 , our approach may miss new writes. Thus, at t_2 , our soft recopy protocol first quiesces the process and recopies the missed writes to ensure correctness (§4.3). CoW is commonly used in fault tolerance cases, where the application can tolerate restoring from a stale state (t_1). On the other hand, recopy is used in cases where the restored process must be resumed from the latest execution (t_2), e.g., live migration (§7).

Both protocols require tracing the process’s *write set*, i.e., which bytes are written during concurrent checkpoint. For CPU writes, we follow the traditional approach to use permission bits in the page table, i.e., write protection for copy-on-write and dirty bits to trace at the page granularity. We omit the detailed CPU-side description since it is well studied. Unfortunately, modern GPUs lack these support, e.g., no hardware dirty bits [27]. Therefore, before delving into our protocols, we first propose a software-based approach to trace GPU writes.

4.1 Tracing GPU write set with validated speculation

Tracing with speculation on GPU API arguments. All operations capable of performing GPU writes are initiated by calling the GPU API, so we intercept these calls to trace the write set. These APIs fall into four categories:

1. Issue memory move operations, e.g., `cudaMemcpy(dst, src, count, ...)`. They write the CPU data (`src`) to the GPU memory (`dst`).
2. Issue communication kernels, e.g., `nccBroadcast(sendbuffer, recvbuffer, count, ...)`. They write the GPU buffers with the content sent through the network.
3. Issue computation kernels with well-defined semantics, e.g., `cublasSgemm(..., A, B, ..., C, ...)`. They perform a computation and update the result buffers (`C`), whose read and write semantics are known in the specifications [52].
4. Issue opaque computation kernels, e.g., `cudaLaunchKernel(func, ... , args, ...)`. They launch kernels written by the developers or just-in-time compiled during runtime, so the reads and writes are unknown to the OS.

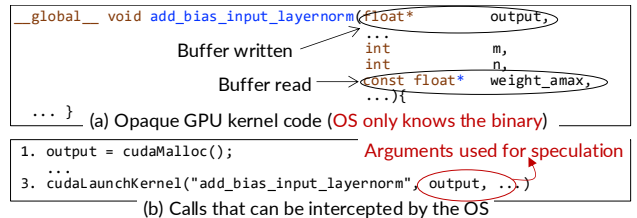


Figure 5: An illustration of the GPU kernel [25] written by the user (a) and how PHOS speculates the accessed buffers (b).

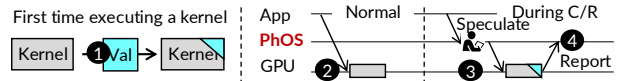


Figure 6: PHOS validation workflow.

For types 1–3 APIs, PHOS directly uses their specifications to trace writes. For instance, the specification of `cudaMemcpy` tells us that executing this API will modify the GPU memory from `dst` to `dst + count`. Empirically, we found over 50% invocations are such APIs (§8.2).

Opaque kernels are trickier because the OS only knows the kernel binary and the arguments invoking it. Our observation is that each GPU kernel represents a clear and straightforward computational purpose whose accessed data addresses are directly encoded in the OS-known arguments calling the kernel. As shown in Figure 5, the data (`output`) written by the kernel is the second argument. Since the OS knows all the buffers allocated by the process by intercepting the GPU memory allocation calls, line 1 (`cudaMalloc`), and it knows each kernel’s function signature [1], we can systematically compare the arguments with the allocated buffers to speculate the buffer written by each kernel.

Specifically, our speculation traces the kernel’s writes at *buffer-level*: When applications launch an opaque GPU computation kernel, for each argument, PHOS treats it as a tentative address pointing to a GPU buffer to write. To decide which buffer is written, we compare it with all the process’s allocated buffers. If the integer value of the argument falls within the range of a buffer, we mark the entire buffer as written. To reduce false positives, we filter out irrelevant arguments with the function signature. Specifically, we use clang [13] to extract the kernel’s argument types, focusing solely on mutable pointer arguments. One type that cannot be precisely filtered out is the C struct type, which is opaque to PHOS as we don’t know the struct definition. For such a type, we conservatively treat all 8-byte chunks in the struct as potential written GPU buffers.

Runtime validation. To handle speculation failures, e.g., extremely rare GPU indirect access (see §8.5), we validate the speculation by instrumenting a runtime validator to the kernel. The validator checks whether each kernel’s GPU memory write instruction falls within the speculated buffers.

Figure 6 presents the validation workflow. When PHOS

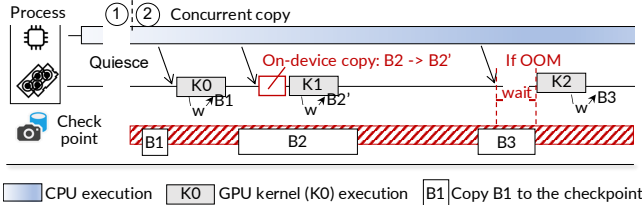


Figure 7: An illustration of the soft copy-on-write protocol for concurrent checkpoint correctness.

encounters an opaque kernel that has not been instrumented (including JIT-compiled ones [58]), it generates a new twin kernel whose kernel binary is the instrumented version of the original kernel binary (❶). The instrumented validator performs the following: For each write instruction, it inserts address range checks before it to verify target address belongs to speculated buffers. If the validation fails, the validator reports the incident to PHOS by writing the address to a pre-allocated PHOS managed CPU buffer. The instrumentation is at the PTX ISA [51]-level for portability. The instrumentation overhead is negligible because for each kernel binary, it will be instrumented only once.

When PHOS intercepts a kernel invocation during checkpoint (❷), it invokes its corresponding instrumented twin kernel. If the kernel reports validation failures, we will execute fallback protocols (described in §4.2 and §4.3) to ensure correctness. The overhead of running the instrumented kernels is also manageable (§8.2) and they are not invoked without checkpoint (❸).

Discussion: the granularity of tracing. Ideally, the trace should be as fine-grained as possible to avoid protocol overhead for ensuring correctness, e.g., avoid excessive copy-on-write. For non-opaque kernels, we can precisely track the bytes written. However, our speculation-based tracing can only detect writes at the buffer-level, which may result in over-tracing. For example, when a kernel only writes a small part of the buffer, we may treat the entire buffer as written. Luckily, such over-tracing is rare especially for recent GPU applications like AI jobs, because (1) AI frameworks (e.g., PyTorch) use a fine-grained buffer allocation, e.g., one for each tensor [59], and (2) the opaque kernels typically write the entire buffer (tensor). See §8.4 for the analysis.

4.2 The GPU soft copy-on-write (CoW) checkpoint

Suppose a checkpoint starts at time t_1 . Our CoW protocol guarantees the final checkpoint matches a stop-the-world checkpoint at t_1 , while allowing concurrent application execution. At a high level, the inconsistency can only happen during execution if the GPU writes to an uncheckpointed buffer. Before we allow such writes to execute, we first copy the data to an on-device buffer, then redirect application writes to a new buffer. Thus, the concurrent checkpoint will not see the new writes.

The protocol. Figure 7 presents the detailed protocol that

consists of two phases: quiesce (❶) and concurrent copy (❷). The quiesce phase stops CPU and GPU execution, the same as existing stop-the-world checkpointing [63, 56]. Note that if we want to checkpoint a multi-process application, the quiesce phase stops all the processes' CPUs and GPUs. Quiescing is necessary because it regulates the current process states to be the same as a possible stop-the-world checkpoint. To quiesce, we first stop CPU to prevent sending new GPU APIs. Then we wait for pending GPU kernels and communications to complete (e.g., via `cudaDeviceSynchronize`). Note that the quiescing overhead is negligible since GPU operations occur at microsecond scales. Thus, despite lacking concurrency, its overhead is significantly lower than data copying (recall Figure 2).

At the copy phase, we copy all the GPU and CPU data to the checkpoint. For CPU data, we follow existing works [73, 66] to isolate concurrent writes with OS's copy-on-write. For GPU, we isolate writes at the GPU API-level: Before executing a GPU kernel (or API), we check whether it writes to a buffer that has not been checkpointed (or is being concurrently checkpointed) using the traced writes through argument-based speculation. If so (e.g., B2), we will first copy the victim buffer to a new buffer allocated on the GPU (B2'), and then redirect the kernel to write to the new buffer (B2'). If multiple concurrent kernels try to write B2, the first kernel will copy B2 to B2', and all the others will wait for the copy to finish before executing on B2'.

Kernel buffer redirection, on-device buffer management and handling mis-speculation. Three things need to be noted. First, redirecting kernel writes to the new buffer is not that trivial: For types 1–3 APIs, we can directly change the arguments for so; but for the opaque ones, we cannot because the arguments can be mis-specified. For example, if the changed argument is not a buffer, the execution will corrupt both application states as well as the checkpoint. Hence, we leave the kernel argument unchanged. To ensure correctness, we copy the buffer to a new on-device buffer, and let the checkpoint copy from the new buffer. A problem is that if an opaque kernel tries to write a buffer that is being concurrently checkpointed, it must be stalled to wait for the checkpoint copy to finish. Since the checkpoint copy is slower than the on-device copy, it may incur extra stalls. Fortunately, we rarely meet such cases empirically due to the low probability of the incidents.

Second, we only reserve a small GPU memory (2 GB) for the copy-on-write, so during CoW we may lack sufficient memory to do the copy. Under such circumstances, we block the kernel until free memory is available (K2 in Figure 7). PHOS does not require a large on-device buffer because once a copy-on-write is done, its original buffer can be released. PHOS achieves so by holistically managing all GPU memory management by extending the related GPU APIs.

Finally, if the validator detects a mis-speculation by reporting a write to a buffer not traced, we will check whether it

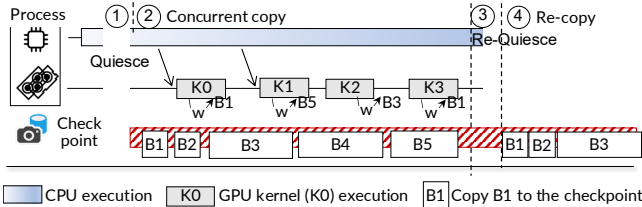


Figure 8: An illustration of the soft dirty buffer protocol for concurrent checkpoint correctness.

affects correctness and react if necessary. If PHOS has checkpointed the buffer before kernel execution, no further action is required. Otherwise, we discard the current checkpoint and retry with a stop-of-the-world approach for liveness. Note that because we don't encounter speculation failures for all major GPU applications, we adopted a simple retry strategy and leave a more advanced one as our future work.

Correctness. Our checkpoint is the same as the resulting checkpoint from a stop-of-the-world checkpoint at the start checkpoint time. First, our quiesce phase is the same as the stop checkpoint. So before the copy phase, our initial process states are the same as a stop checkpoint. Second, during our concurrent copy, we only copy the states not modified by concurrent execution, because all writes are isolated by copy-on-write. As the stop checkpoint also faithfully checkpoints the same state, our checkpoint is the same as its checkpoint.

4.3 The GPU soft recopy checkpoint

Suppose the concurrent checkpoint starts at t_1 and the data copy ends at t_2 . Our recopy protocol recopies the written buffers during concurrent copy to ensure the checkpoint is the same as the stop-the-world checkpoint at t_2 .

The protocol. Figure 8 presents how the protocol executes, which contains four phases. The first quiesce phase (①) stops all the CPU and GPU execution, the same as the CoW protocol, ensuring that during concurrent copy, we will not miss tracing any writes. Afterward, PHOS resumes application execution, and copies the CPU and GPU data to the checkpoint (②). During the concurrent copy, before launching a kernel (or an API), we trace the buffers written by the kernel using the speculation and validation method. For each buffer, we will check whether it is dirty, i.e., the buffer has been checkpointed or is being checkpointed. If dirty, we will add it to a dirty buffer set for recopy. In the Figure 8 example, B1 and B3 are dirty but B5 is not. The CPU dirty pages are tracked via page table's dirty bit.

Once all the data has been copied, we start another quiesce phase to stop the CPU and GPU execution (③). Note that dirty buffers written during the quiesce phase will also be recorded. After the quiesce is done, we recopy all the GPU dirty buffers CPU dirty pages to the checkpoint (④). The application is stopped to ensure correctness, but we can also iteratively do the concurrent recopy similar to CPU-based protocols [14].

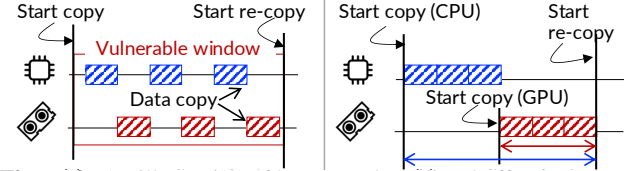


Figure 9: An illustration of how to reduce dirty buffers generated by prioritized CPU and GPU concurrent checkpoint. Note that the bars only show the execution on CPU and GPU, not the time when the dirty buffers can be generated.

Handling mis-speculation. Handling speculation failures is simple for recopy: if the speculation is wrong, the validator will return the victim buffers such that we can add them to the dirty buffer set if they are dirty.

Correctness. Assume the concurrent copy completes at t_2 . We will show that our checkpoint matches a stop checkpoint at t_2 . First, it is straightforward to see that the re-quiesce and recopy phases (③ + ④) are nearly identical to a stop checkpoint at t_2 . The only difference is that we only copy the dirty buffers. To remedy, we use the buffers copied during ② for the remaining buffers. It is correct to do so because buffers not recopied are the same as when doing a stop checkpoint at t_2 because they are not dirty. Thus, combining buffers copied from the two phases results in the same checkpoint as obtained from a stop checkpoint at t_2 .

5 Making concurrent GPU checkpoint fast

While concurrent checkpoint can effectively minimize the process stalls, efficiently realizing it requires addressing several technical issues.

Reducing dirty buffers via coordinated GPU and CPU checkpoint. In the soft recopy protocol, the timing of the copy is critical to reducing the number of dirty buffers: if the copy is performed after the kernel write, the buffer will not become dirty so it will not be recopied. This requires copying buffers that are unlikely to be written first.

In GPU processes, we found the data written by the CPU and GPU differ: GPU writes more data than CPU. Thus, it is beneficial to first copy the CPU data instead of copying the GPU data, as shown in Figure 9 (b). However, naively checkpointing the CPU data and GPU data without control cannot achieve the aforementioned goal, because CPU and GPU checkpoints share the checkpoint bandwidth and thus interfere with each other (see Figure 9 (a)). Thus, we implement a coordinated checkpoint in our checkpoint engine: we first copy the CPU data, then the GPU data.

Prioritized application PCIe transfer. When we completed our first concurrent checkpoint implementation (for both protocols), we found the process still stalls during the checkpoint. By profiling the utilization of GPU hardware, we found it is because the checkpoint data copy has saturated the GPU PCIe transfer engines. Specifically, GPUs have a limited number

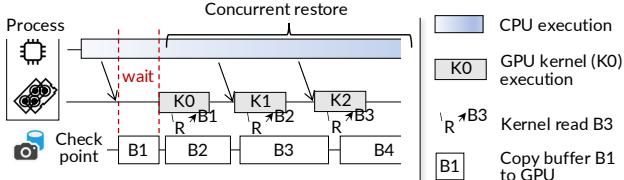


Figure 10: An illustration of the concurrent restore in PHOS.

of PCIe transfer engines [7] shared between PHOS and applications. Without control, the bulk checkpoint load could easily saturate the PCIe engine, causing application execution starvation if it needs to load data from PCIe.

To this end, we adopt two techniques to avoid application starvation—the goal is to prioritize application PCIe transfer over the checkpoint, observing that applications infrequently use the PCIe but such usages are on their critical path. First, we intercept all process’s PCIe-related API calls (e.g., `cudaMemcpy`) to detect application PCIe transfer. Second, we implemented a preemption mechanism by using chunk-based checkpoint data copy. Specifically, for each GPU buffer, we copy it to the checkpoint in small 4 MB chunks. After copying one chunk, we check whether there is ongoing or pending application transfer. If so, we pause the checkpoint copy and let the pending application transfers execute first.

6 Concurrent GPU restore

Concurrent and correct restore. When restoring data from the checkpoint to the GPUs, PHOS allows processes execution concurrently when PHOS is copying data from the checkpoint to the GPU buffers. Figure 10 illustrates the execution flow. To ensure correctness, before executing a kernel (or API), we check whether the data it requires has been copied or not. If not, we pause the execution, copy the buffer containing the required data on demand, and then resume. In our example, K0 will wait for B1 to be copied. If the data has been copied, e.g., K1 and K2, kernels can execute while the restore is concurrently executing (copying B3 and B4). This effectively overlaps computation with data transfer, reducing the observable impact of data copy overhead analyzed in §2.3.

Recall from §4 that the checkpoint of PHOS is correct. Given this guarantee, the correctness of concurrent restore depends on accurately tracing execution’s read set, similar to prior CPU systems [72, 20, 69]. We describe it next.

Tracing GPU read set with extended speculation with validation. PHOS extends the argument-based speculation described in §4.1 to speculate the data read by launching a piece of GPU execution with API calls. The extension is simple: we treat launch arguments declared as immutable pointers (e.g., `const void *`) as tentative read buffers required. Note that we still need to trace writes here, because GPU kernels may perform partial writes to buffers.

Handling mis-speculation. Like writes, we also instrument a validator to ensure correctness under speculation failures.

If the speculation is wrong, the validator will notify PHOS to handle. On the other hand, the mis-speculation handling is more complex, because the kernel may have accessed inconsistent GPU states caused by a partially restored buffer. To ensure correctness, we must roll back the GPU states to a correct state. Our current solution rolls back to the initial state from the checkpoint and then performs a stop-of-the-world restore for liveness. We choose this simple solution because we have not met speculation failures in common GPU applications. While a more efficient solution could involve isolating partial updates using our soft copy-on-write protocol, we defer this optimization for future work.

Accelerate restore with context pool. The final challenge for implementing concurrent restore is that GPU context creation must precede kernel execution and buffer copying, as the context initialization involves setting up GPU memory subsystems. This initialization incurs comparable overhead to data copy, as analyzed in §2.3.

To address the issue, our key observation is that GPU execution is decoupled from the context it uses: a process can use any context capable of execution. Therefore, we pre-create a pool of common GPU contexts at PHOS. Specifically, we maintain the pool in the PHOS daemon—a long-running OS service that pre-creates CUDA and cuBLAS contexts with `cuCtxCreate` and `cublasCreate` at boot time. For multi-GPU applications, we also pre-create an NCCL group communicator that covers all GPUs connected via NVLink, which can accelerate establishing the NCCL group communicator with sub-topology using `ncclCommSplit` [47] efficiently. We don’t create communicators across machines because the ideal communicator may depend on the network topology. The context pool operates in a separate process space, so applications must use inter-process communication mechanisms to access it.

With the context pool in PHOS daemon, when a GPU process requests to create a context, we intercept the context creation API call and assigns a pre-existing context from the pool. We also track the mapping between the context and the GPU process, ensuring all subsequent GPU API calls from that process utilize the mapped context.

7 Empowering applications with PHOS

Providing fault tolerance to GPU processes (Checkpoint mostly). Distributed computing applications such as training are susceptible to GPU failures [26, 22, 63]. PHOS provides transparent fault tolerance through periodic GPU process checkpointing using our soft copy-on-write (CoW) protocol described in §4.2. The checkpoints are stored in fast fault-tolerant storage, such as replicated remote memory [71]. If a failure occurs, PHOS stops all GPU processes, and then restores them from the most recent checkpoint. The checkpoint frequency is determined by holistically considering both the checkpoint overhead as well as the loss of computation due to

Table 2: Applications evaluated. * indicates a multi-GPU setup. PPO is training-only, and our setup cannot run Llama-3-70B training.

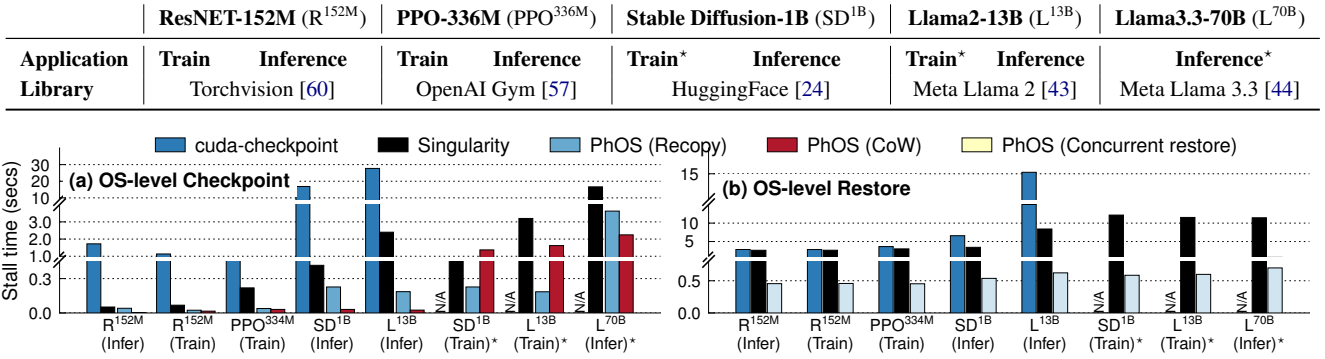


Figure 11: The application stall time caused by different OS-level checkpoint and restore systems.

restoring from a stale checkpoint, similar to prior work [28]. The detailed method is left in the appendix (§A.1). For fault tolerance, using a slightly stale checkpoint (i.e., one that does not capture the absolute latest execution state) is acceptable, because the latest state can be recovered through recomputation after restoring.

Two things to note. First, fault tolerance is a checkpoint-mostly case, as the checkpoint frequency is high to avoid losing computation results [71]. In comparison, the restore only happens upon failures, which occur much less frequently [46, 78]. Second, we need to ensure the checkpoint from all the involved processes is consistent [63]. Thus, we extended the quiescing phase described in §4.2 across all involved processes. After the quiesce, we can checkpoint each process with CoW separately.

Live migration of a GPU process (Checkpoint + Restore). PHOS implemented pre-copy-style live migration [14]: It first checkpoints the process via our recopy protocol, then restores it on the target node. The recopy protocol is necessary because the destination should resume exactly at the last execution state at the source node. To avoid redundant data copy from first copying the data from source GPU to the checkpoint, then from the checkpoint to the target GPU, we use GPU-direct RDMA [2] to directly copy the data from the source GPUs’ buffers to the target GPUs’ buffers.

Fast GPU serverless function startups (Restore mostly). In serverless computing, processes are created on demand for each request [33, 16]. Since each process has an entry function to react to a request, we take a checkpoint before the entry. Afterward, once a request comes, we restore the process from the checkpoint using our concurrent restore protocol described in §6. This eliminates the overhead to run till the entry function (commonly termed coldstart costs) [72, 5].

8 Evaluation

We have implemented PHOS in 54,839 LoC in C++ and Rust, excluding the CUDA GPU driver extension framework, communication libraries and integration with CRIU [18].

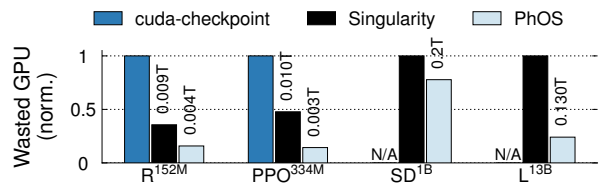


Figure 12: The average wasted GPU time (normalized) using different checkpoint methods for fault tolerance on training workloads. The wasted time is normalized to the total time used for training (T), and the displayed time is normalized to the number of systems with the maximum wasted time for ease of interpretation. cuda-checkpoint does not support checkpointing distributed jobs.

Testbed. We conducted our experiments on two servers, each with eight NVIDIA A800 (80 GB HBM and 400 Gbps NVLink interconnects) GPUs, two Intel Xeon Gold 6348 CPUs (total 56 cores), and 1 TB of DRAM. Two servers are connected via an RDMA network with 100 Gbps bandwidth between each GPU and install CUDA 12.3 [48].

Baselines. We compare PHOS with NVIDIA’s official OS-level checkpoint and restore tool—cuda-checkpoint [56]. Nevertheless, we found it is extremely slow, e.g., it cannot achieve a PCIe-fully utilized data copy speed, see Figure 11. Yet, we don’t have its source code to analyze. To compare with the best performance of the stop-the-world C/R, we implemented Singularity [63]—the state-of-the-art stop-the-world GPU C/R system, in our codebase as the baseline. We have carefully tuned the implementation, e.g., we leverage pinned memory to achieve maximum data copy performance, to ensure a fair comparison with PHOS. As shown in Figure 11, our implementation of Singularity has orders of magnitude smaller application stall time than cuda-checkpoint. Thus, we will omit a detailed comparison with cuda-checkpoint in later analysis. Finally, a recent work CRIUgpu [64] builds on cuda-checkpoint to support a unified stop-the-world checkpoint and restore. Its objective is for functionalities but not performance. Hence, we omit a comparison because it has the same performance as cuda-checkpoint.

Evaluated applications. We focus on evaluating AI applications—the dominated GPU applications to show the

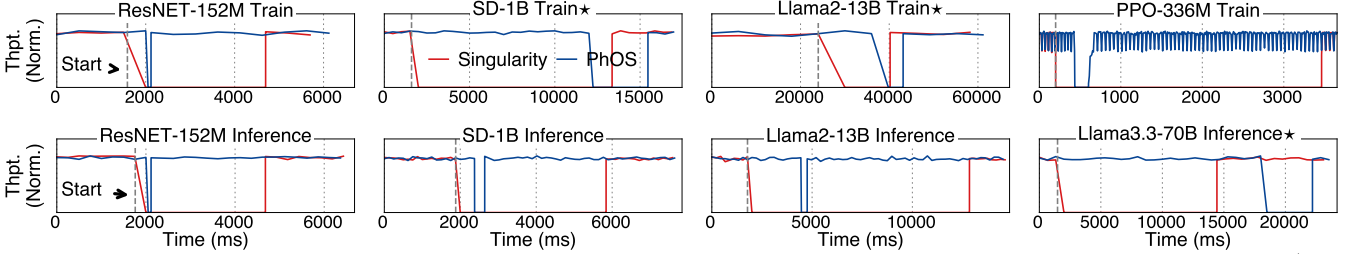


Figure 13: The downtime of migrating processes between machines with different systems. Multi-GPU workloads are marked with *.

effectiveness of PHOS. Table 2 summarizes the evaluated applications. We choose workloads of both training and inference, whose domains span vision tasks (ResNet), large foundational models (Llama2-13B and Llama3.3-70B), and reinforcement learning (PPO). These tasks may either use one or multiple GPUs. We follow the common setups for running these applications, and leave the detailed setup descriptions in the appendix (§A.3) due to space limitation.

8.1 End-to-end application performance

We choose the end-to-end C/R workloads described in §7 to evaluate the effectiveness of PHOS.

Fault tolerance: evaluated metrics and results. To evaluate the fault tolerance performance of PHOS, we choose training applications and compare the performance of PHOS with baselines. Following existing works [71, 28], we compare the following metrics: checkpoint overhead and wasted GPU time during training. The checkpoint overhead measures the stall time caused by checkpointing, while the wasted GPU time is measured by the end-to-end training GPU time wasted when compared to an unrealistic, non-fault execution. The checkpoint is stored in host memory to avoid slow storage [71].

Figure 11 (a) measures the checkpoint overhead, with the checkpoints done at the beginning of the iteration. The stall is calculated by first subtracting the total training time with and without the checkpoint and then normalized to a single iteration time. We can see that PHOS reduced the checkpoint overhead by 70–160% compared to Singularity thanks to the concurrent checkpoint. Notably, on Llama2-13B training, the overhead of PHOS is only 185 ms, while Singularity is 3.2 s, bottlenecked by transferring the checkpoint data (72 GB) to the host memory (32 GBps PCIe). For reference, the iteration time is 6.9 s.

Figure 12 further compares the average wasted GPU hours with the optimal checkpoint frequency, whose formula is listed in §A.1, the same as a priori work [28]. Since the wasted time is related to the failure frequency, we set a failure ratio of one GPU fails per hour reported by various industry reports [78, 46]. The results show that PHOS saves up to 22–86% GPU hours compared with other approaches. This is because PHOS enables a higher checkpoint frequency to save wasted GPU hours due to recomputation. For example, in Llama2-13B training, PHOS enables a checkpoint frequency of 279 per hour, while the optimal setup for Singularity is 67.

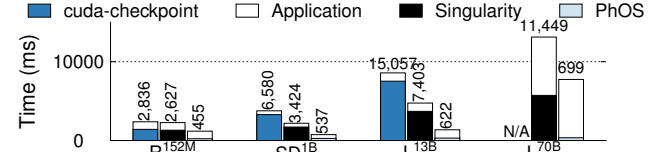


Figure 14: The serverless function execution time under coldstart. The Exe. states for the function execution time. All the workloads are inference.

Live migration: evaluated metric and results. To evaluate the effectiveness of PHOS in live migration scenarios, we measure the downtime when migrating applications between nodes. Figure 13 shows the timeline of application performance during migration. The results show that PHOS incurs a minimal downtime thanks to the concurrent execution capabilities. Notably, PHOS only incurs 3.3 and 3.7 seconds of downtime for migrating Llama2-13B training and Llama2-70B inference, respectively. In comparison, Singularity incurs 10.2 and 12.35 seconds of downtime, which is dominated by copying data from the source GPU to the target. In Llama2-13B training, copying data through 100 Gbps RDMA takes at least 9.8 seconds.

Serverless function startup: evaluated metric and results. We evaluate the effectiveness of PHOS in GPU serverless workloads by measuring the end-to-end execution time, i.e., considering both startup and application function execution time [5, 20]. We stored the function checkpoint in host DRAM and measured the execution time under cold start with OS-level restore. We choose inference workloads because training workloads are stable and do not need serverless-style startup. Figure 14 shows the results: PHOS has the fastest execution time: on average, it improves upon cuda-checkpoint and Singularity by 24× and 16× respectively, thanks to the eliminated GPU context creation time as well as its ability to overlap copying data stalls with concurrent restore.

8.2 Performance breakdown and ablation study

Breakdown of the copy-on-write protocol. Figure 16 shows the breakdown of the checkpoint stall caused by different checkpoint methods on a Llama2-13B training workload. Other workloads share a similar trend. All the system checkpoints at the beginning of the iteration: the optimal checkpoint timing, as analyzed in §8.3. We can see that first, though the

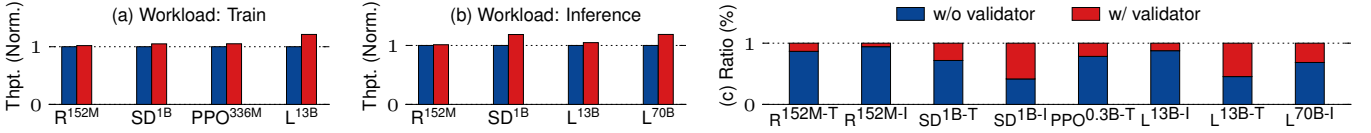


Figure 15: An analysis of the runtime validator overhead on (a) training and (b) inference workloads. (c) Analysis of the ratios of the kernels instrumented with the validator. -T is abbreviated for training while -I is for inference.

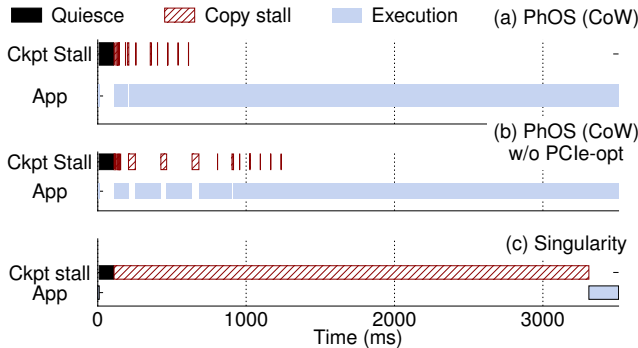


Figure 16: A breakdown of the checkpoint overhead on (a) PHOS CoW, (b) without our prioritized PCIe transfer optimization and (c) Singularity. Workload: Llama2-13B Training*. Note that we omitted the concurrent data copy of PHOS.

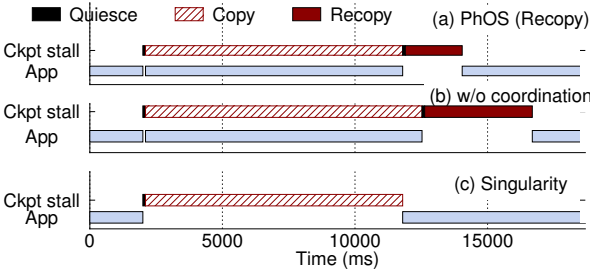


Figure 17: A breakdown of the checkpoint overhead on (a) PHOS recopy, (b) without our coordinated CPU GPU checkpoint optimization and (c) Singularity. Workload: Llama2-70B Inference*. Note that we omitted the concurrent data copy of PHOS.

quiescing phase will stop the application execution, its absolute time (10 ms) is extremely small so this phase has a negligible overhead. The absolute time is small because (1) ongoing kernels are short-lived and (2) coordinating between threads with RDMA to reach a global quiesce is extremely efficient. Second, though PHOS may stall application due to copy-on-write, the aggregated stalls are small as long as PHOS can timely finish the data copy.

Effectiveness of the prioritized application PCIe transfer. We further evaluate the effectiveness of our prioritized application PCIe transfer optimization described in §5. As shown in Figure 16, without this optimization (b), applications still suffers stalls due to PCIe bandwidth competition, even when they have not written data that may cause an incorrect checkpoint (a). This is because the GPU kernels are waiting to load the training set from the CPU, which is blocked by the checkpoint data copy due to the limited number of GPU DMA engines on the GPUs.

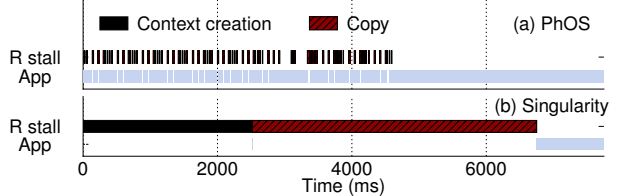


Figure 18: A breakdown of the restore on (a) PHOS concurrent restore, and (b) Singularity. Workload: Llama2-13B inference. Note that we omitted the concurrent data copy of PHOS. R stall states for restore stall time.

Breakdown of the recopy protocol. Figure 17 shows the breakdown of executing our recopy protocol on a Llama2-70B inference workload*. We can see that the downtime of PHOS is dominated by the recopy time. The downtime is longer for recopy when compared with CoW because it not only ensures that the checkpoint is correct, but it is also fresh. Nevertheless, the downtime is still orders of magnitude smaller than a stop-the-world approach (Singularity) because the recopied data is orders of magnitude smaller (2.1 vs. 9.7 seconds).

Effectiveness of the coordinated CPU and GPU checkpoint. Figure 17 further evaluates the effectiveness of our coordinated CPU and GPU checkpoint optimization in §5, aiming to reduce the amount of data for the recopy phase. Thanks to the optimized GPU concurrent copy timing, PHOS enjoys 47% smaller recopy time than without optimization (b). The recopied data reduces from 50 to 27 GB per GPU. Since the copy is a bulk load procedure, the reduced transferred size directly translates to a smaller recopy time.

Breakdown of the concurrent restore. Figure 18 shows the breakdown of concurrent restoring a Llama2-13B inference process using PHOS. We can see that compared to the stop-the-world restore (b), the improvements of PHOS come from two factors: (1) the eliminated context creation and (2) overlapping the data copy with the kernel execution. Note that during application execution, PHOS still copies the data in the background: this perfectly aligns with how inference processes access data nowadays: before executing the first layer of inference, we can concurrently restore the second layer’s data. Unlike previous work [75, 6], PHOS achieves so transparently.

The runtime overhead of tracing GPU read and write set. Figure 15 (a) and (b) report the runtime overhead of runtime validator on different applications. We observe a relatively small slowdown of 1–12% for various workloads. The observable overhead is small because: (1) the additional check only

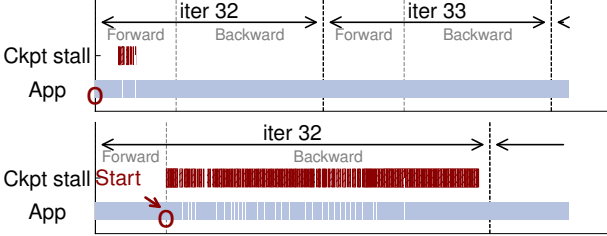


Figure 19: Impact of checkpoint timing on the performance of Llama2-13B training. The blank in App is the stalled caused by the CoW. The red indicates the data copy time. Note that we omitted the concurrent data copy of PHOS.

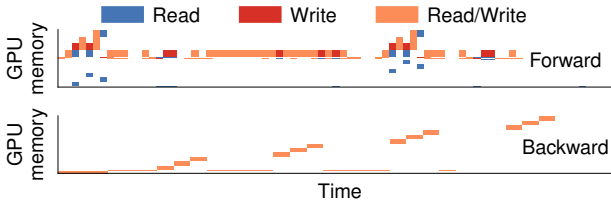


Figure 20: A heatmap showing the read and write sets traced by our speculated validation method on a Llama2-13B training workload.

happens when the kernel accesses the global memory, which is less frequent for high computational efficiency; and (2) the instrumented kernels are only a small portion of the overall kernels in the workloads, as shown in Figure 15 (c).

8.3 Impact of checkpoint timing on performance

Figure 19 analyzes how the checkpoint timing affects the performance of PHOS on the CoW protocol. We omit analysis on the recopy protocol as it is similar. We control the timing with our SDK (see §A.2). We run LLama2-13B training workload and choose two times: (1) at the beginning of an iteration (before the forward pass), (2) at the end of the iteration (at the update phase). We measure the performance specifically on the 32th iteration to fully warm up the application. We can see that checkpoint at (1) is more efficient because few buffers are updated at the beginning: only activation buffers are updated (see also §8.4). Thus, if we can finish the checkpoint before reaching the update pass, we meet few stalls due to CoW. In (1), copy 2.3 GB of data via 32 GBps PCIe¹ takes 185 ms, while the iteration time is 6.3 s.

8.4 A close look at GPU read and write traced by PHOS

Figure 20 reports the GPU accesses traced by PHOS on Llama2-13B training. First, we can see that though PHOS traces accesses at buffer level, it is still fine-grained enough to support an efficient CoW and recopy, because GPU applications typically allocate and write buffers in a fine-grained way. Moreover, the access patterns differ across different phases of execution, so the checkpoint timing is important.

¹The measured bandwidth is 25 GBps, slightly below the hardware limit.

Table 3: A study of the success rate of our speculation-based GPU read and write sets tracing beyond our evaluated applications.

GPU Apps	#kernels/failed	#Instances/failed
Rodinia [10]	44 / 1	48,610 / 20
Parboil [65]	18 / 0	43,473 / 0
vLLM [35]	66 / 0	13,625 / 0
TVM [11]	607 / 0	186,244 / 0
FlashInfer [3]	69 / 0	15,265 / 0

8.5 A study of the feasibility of speculation

For all the common GPU applications evaluated by PHOS, we don’t meet any speculation failure. To evaluate the feasibility of our speculation, we conduct a comprehensive study across diverse GPU applications including supercomputing workloads (Rodinia [10] and Parboil [65]), dynamically generated kernels from AI compilers (TVM [11]), and highly optimized handwritten kernels (vLLM [35] and FlashInfer [3]) in Table 3. To evaluate the success rate of our speculation, we run typical tasks provided by them (we term each task *instance*). For Rodinia and Parboil, we ran all benchmarks except for ones that had bugs or used outdated CUDA APIs (e.g., dwt2d). For TVM, we ran inference on their available models other than our previous evaluated (e.g., DenseNet, YOLOv4). Out of all instances, only one kernel (from Rodinia) failed our speculation—a fairly dated supercomputing application. The failure occurred because it reads a buffer pointed to by a global variable not listed in the arguments.

9 Discussion

Supporting advanced GPU features like CUDA graph. CUDA graph [4] allows the CPU to submit a batch of kernels. PHOS supports tracing reads and writes of kernels with CUDA graph, inspired by Medusa [77]. Specifically, CUDA graphs can be utilized as follows: (1) explicitly invoking APIs such as `cudaGraphAddKernelNode`, or (2) implicitly constructing them through the driver using `cudaStreamBeginCapture`. Both methods require explicit driver API calls, so they are compatible with our speculative approach.

GPU hardware extensions and OS-level ABI for concurrent C/R. PHOS is the first system to show the effectiveness of concurrent GPU checkpoint and restore as well as how to realize it in major GPUs. While hardware extensions like GPU dirty bit could simplify and accelerate PHOS’s implementation, they are less flexible, e.g., a hardware dirty bit alone cannot support our other protocols like soft copy-on-write. On the other hand, an OS-level ABI enabling developers to specify kernel buffer access patterns would fully utilize PHOS’s capabilities. Yet modifying numerous existing custom kernels to adopt this ABI is non-trivial. How to develop systematic fine-grained kernel memory access tracing methods beyond our speculative approach is left as our future work.

10 Related work

Checkpoint and restore. PHOS continues the line of research on C/R, with a focus on efficient OS-level GPU C/R [21, 41, 29, 62, 66, 18, 36, 30, 73, 64], a feature currently only available on CPU. A recent work (whose submission time is 2 months after our first released preprint²)—gCROP [75], uses concurrent restore to accelerate process startup (only) on AMD GPUs. They ensure concurrent restore correctness with significant application modifications, which PHOS achieves the same effect without application modifications using our novel validated speculation. They cannot support multiple GPUs, their approach is infeasible on NVIDIA GPUs, and most importantly, they don’t support concurrent checkpoint—though their paper title misleadingly claims so. GPU snapshot [37] realizes dirty bit with simulated GPU hardware extension, which to the best of our knowledge, no real hardware implementation exists. PHOS is the only system that supports both concurrent OS-level checkpoint and restore for GPU applications on multi-GPU and major GPU vendors (i.e., NVIDIA GPUs).

Analyzing GPU kernels. Many existing works analyze GPU programs (kernels), either statically or during runtime [12, 39, 8, 9, 34, 38, 40, 42]. PHOS takes a different approach: instead of analyzing the program, we analyze the kernel arguments for speculation. This avoids the incompleteness inherent in GPU kernel analysis (as GPU kernels are Turing complete) and works well for concurrent GPU checkpoint and restore.

11 Conclusion

We contribute the first concurrent OS-level GPU checkpointing and restoring system using validated speculation, and demonstrate its effectiveness in various critical downstream applications, including fault tolerance, live migration, and fast startup. Our current prototype is built on NVIDIA GPUs, but our methodologies are generalizable to other accelerators, and we plan to support these devices in the future.

Acknowledgment

We would like to thank the reviewers from SOSP’24, OSDI’24 and SOSP’25 for their insightful feedback. We sincerely thank Zhiyuan Dong, Dingyan Zhang and Xiating Xie for giving us feedback on the early draft of this paper. We would also like to thank Shaoxun Zeng for sharing details on how PHOS can be adapted to support CUDA graph. This work was supported in part by the National Key Research & Development Program of China (No. 2022YFB4500700), the Fundamental Research Funds for the Central Universities, the National Natural Science Foundation of China (No. 62202291, 62272291), as well as a research grant from Huawei.

²<https://arxiv.org/abs/2405.12079>

References

- [1] cu++filt. <https://docs.nvidia.com/cuda/cuda-binary-utilities/index.html#cu-filt>, 2025.
- [2] Developing a linux kernel module using gpudirect rdma. <https://docs.nvidia.com/cuda/gpudirect-rdma/>, 2025.
- [3] FlashInfer: Kernel Library for LLM Serving. <https://github.com/flashinfer-ai/flashinfer>, 2025.
- [4] Getting started with cuda graphs. <https://developer.nvidia.com/blog/cuda-graphs/>, 2025.
- [5] AO, L., PORTER, G., AND VOELKER, G. M. Faasnap: Faas made fast using snapshot-based vms. In *EuroSys ’22: Seventeenth European Conference on Computer Systems, Rennes, France, April 5 - 8, 2022* (2022), Y. Bromberg, A. Kermarrec, and C. Kozyrakis, Eds., ACM, pp. 730–746.
- [6] BAI, Z., ZHANG, Z., ZHU, Y., AND JIN, X. PipeSwitch: Fast pipelined context switching for deep learning applications. In *14th USENIX Symposium on Operating Systems Design and Implementation (OSDI 20)* (Nov. 2020), USENIX Association, pp. 499–514.
- [7] BAKITA, J., AND ANDERSON, J. H. Demystifying nvidia gpu internals to enable reliable gpu management.
- [8] BETTS, A., CHONG, N., DONALDSON, A. F., KETEMA, J., QADEER, S., THOMSON, P., AND WICKERSON, J. The design and implementation of a verification technique for GPU kernels. *ACM Trans. Program. Lang. Syst.* 37, 3 (2015), 10:1–10:49.
- [9] BETTS, A., CHONG, N., DONALDSON, A. F., QADEER, S., AND THOMSON, P. Gpuverify: a verifier for GPU kernels. In *Proceedings of the 27th Annual ACM SIGPLAN Conference on Object-Oriented Programming, Systems, Languages, and Applications, OOPSLA 2012, part of SPLASH 2012, Tucson, AZ, USA, October 21-25, 2012* (2012), G. T. Leavens and M. B. Dwyer, Eds., ACM, pp. 113–132.
- [10] CHE, S., BOYER, M., MENG, J., TARJAN, D., SHEAFFER, J. W., LEE, S., AND SKADRON, K. Rodinia: A benchmark suite for heterogeneous computing. In *Proceedings of the 2009 IEEE International Symposium on Workload Characterization, IISWC 2009, October 4-6, 2009, Austin, TX, USA* (2009), IEEE Computer Society, pp. 44–54.
- [11] CHEN, T., MOREAU, T., JIANG, Z., ZHENG, L., YAN, E. Q., SHEN, H., COWAN, M., WANG, L., HU, Y., CEZE, L., GUESTRIN, C., AND KRISHNAMURTHY, A. TVM: an automated end-to-end optimizing compiler for deep learning. In *13th USENIX Symposium on Operating Systems Design and Implementation, OSDI 2018, Carlsbad, CA, USA, October 8-10, 2018* (2018), A. C. Arpaci-Dusseau and G. Voelker, Eds., USENIX Association, pp. 578–594.
- [12] CHIANG, W., GOPALAKRISHNAN, G., LI, G., AND RAKAMARIC, Z. Formal analysis of GPU programs with atomics via conflict-directed delay-bounding. In *NASA Formal Methods, 5th International Symposium, NFM 2013, Moffett Field, CA, USA, May 14-16, 2013. Proceedings* (2013), G. Brat, N. Rungta, and A. Venet, Eds., vol. 7871 of *Lecture Notes in Computer Science*, Springer, pp. 213–228.
- [13] CLANG. Clang: a c language family frontend for llvm, 2024.

[14] CLARK, C., FRASER, K., HAND, S., HANSEN, J. G., JUL, E., LIMPACH, C., PRATT, I., AND WARFIELD, A. Live migration of virtual machines. In *2nd Symposium on Networked Systems Design and Implementation NSDI (2005), May 2-4, 2005, Boston, Massachusetts, USA, Proceedings* (2005), A. Vahdat and D. Wetherall, Eds., USENIX.

[15] CLOUD, A. <https://developer.aliyun.com/article/1610603>, 2024.

[16] CLOUD, A. Serverless gpu overview. <https://www.alibabacloud.com/tech-news/a/serverless/4o2cc4hux4q-serverless-gpu-overview>, 2024.

[17] CRIU. Tcp repair mode in kernel.

[18] CRIU. Criu main page, 2024.

[19] CRIU. Memory changes tracking. https://criu.org/Memory_changes_tracking, 2025.

[20] DU, D., YU, T., XIA, Y., ZANG, B., YAN, G., QIN, C., WU, Q., AND CHEN, H. Catalyster: Sub-millisecond startup for serverless computing with initialization-less booting. In *ASPLOS '20: Architectural Support for Programming Languages and Operating Systems, Lausanne, Switzerland, March 16-20, 2020* (2020), J. R. Larus, L. Ceze, and K. Strauss, Eds., ACM, pp. 467–481.

[21] EGWUTUOHA, I. P., LEVY, D., SELIC, B., AND CHEN, S. A survey of fault tolerance mechanisms and checkpoint/restart implementations for high performance computing systems. *The Journal of Supercomputing* 65, 3 (2013), 1302–1326.

[22] EISENMAN, A., MATAM, K. K., INGRAM, S., MUDIGERE, D., KRISHNAMOORTHI, R., NAIR, K., SMELYANSKIY, M., AND ANNAVARAM, M. Check-n-run: a checkpointing system for training deep learning recommendation models. In *19th USENIX Symposium on Networked Systems Design and Implementation, NSDI 2022, Renton, WA, USA, April 4-6, 2022* (2022), A. Phanishayee and V. Sekar, Eds., USENIX Association, pp. 929–943.

[23] ELNOZAHY, E. N., ALVISI, L., WANG, Y., AND JOHNSON, D. B. A survey of rollback-recovery protocols in message-passing systems. *ACM Comput. Surv.* 34, 3 (2002), 375–408.

[24] FACE, H. The ai community building the future. <https://huggingface.co>, 2024.

[25] FASTERTRANSFORMER. Nvidia, 2024.

[26] GAO, Y., SHI, X., LIN, H., ZHANG, H., WU, H., LI, R., AND YANG, M. An empirical study on quality issues of deep learning platform. In *45th IEEE/ACM International Conference on Software Engineering: Software Engineering in Practice, SEIP@ICSE 2023, Melbourne, Australia, May 14-20, 2023* (2023), IEEE, pp. 455–466.

[27] GUO, Y., ZHANG, Z., AND YANG, J. GPU memory exploitation for fun and profit. In *33rd USENIX Security Symposium, USENIX Security 2024, Philadelphia, PA, USA, August 14-16, 2024* (2024), D. Balzarotti and W. Xu, Eds., USENIX Association.

[28] GUPTA, T., KRISHNAN, S., KUMAR, R., VIJEEV, A., GULAVANI, B. S., KWATRA, N., RAMJEE, R., AND SIVATHANU, M. Just-in-time checkpointing: Low cost error recovery from deep learning training failures. In *Proceedings of the Nineteenth European Conference on Computer Systems, EuroSys 2024, Athens, Greece, April 22-25, 2024* (2024), ACM, pp. 1110–1125.

[29] HARDY, N. Keykos architecture. *SIGOPS Oper. Syst. Rev.* 19, 4 (oct 1985), 8–25.

[30] HARGROVE, P. H., AND DUELL, J. C. Berkeley lab checkpoint/restart (blcr) for linux clusters. In *Journal of Physics: Conference Series* (2006), vol. 46, IOP Publishing, p. 067.

[31] JIANG, Z., LIN, H., ZHONG, Y., HUANG, Q., CHEN, Y., ZHANG, Z., PENG, Y., LI, X., XIE, C., NONG, S., JIA, Y., HE, S., CHEN, H., BAI, Z., HOU, Q., YAN, S., ZHOU, D., SHENG, Y., JIANG, Z., XU, H., WEI, H., ZHANG, Z., NIE, P., ZOU, L., ZHAO, S., XIANG, L., LIU, Z., LI, Z., JIA, X., YE, J., JIN, X., AND LIU, X. MegaScale: Scaling large language model training to more than 10,000 GPUs. In *21st USENIX Symposium on Networked Systems Design and Implementation (NSDI 24)* (Santa Clara, CA, Apr. 2024), USENIX Association, pp. 745–760.

[32] JOHNSON, E. Starting up faster with aws lambda snap-start. <https://aws.amazon.com/cn/blogs/compute/starting-up-faster-with-aws-lambda-snapstart/>, 2024.

[33] JONAS, E., SCHLEIER-SMITH, J., SREEKANTI, V., TSAI, C., KHANDELWAL, A., PU, Q., SHANKAR, V., CARREIRA, J., KRAUTH, K., YADWADKAR, N. J., GONZALEZ, J. E., POPA, R. A., STOICA, I., AND PATTERSON, D. A. Cloud programming simplified: A berkeley view on serverless computing. *CoRR abs/1902.03383* (2019).

[34] KAMATH, A. K., AND BASU, A. iguard: In-gpu advanced race detection. In *SOSP '21: ACM SIGOPS 28th Symposium on Operating Systems Principles, Virtual Event / Koblenz, Germany, October 26-29, 2021* (2021), R. van Renesse and N. Zeldovich, Eds., ACM, pp. 49–65.

[35] KWON, W., LI, Z., ZHUANG, S., SHENG, Y., ZHENG, L., YU, C. H., GONZALEZ, J., ZHANG, H., AND STOICA, I. Efficient memory management for large language model serving with pagedattention. In *Proceedings of the 29th Symposium on Operating Systems Principles, SOSP 2023, Koblenz, Germany, October 23-26, 2023* (2023), J. Flinn, M. I. Seltzer, P. Druschel, A. Kaufmann, and J. Mace, Eds., ACM, pp. 611–626.

[36] LAADAN, O., AND HALLYN, S. E. Linux-cr: Transparent application checkpoint-restart in linux. In *Linux Symposium* (2010), vol. 159, Citeseer.

[37] LEE, K., SULLIVAN, M. B., HARI, S. K. S., TSAI, T., KECKLER, S. W., AND EREZ, M. GPU snapshot: checkpoint offloading for gpu-dense systems. In *Proceedings of the ACM International Conference on Supercomputing, ICS 2019, Phoenix, AZ, USA, June 26-28, 2019* (2019), R. Eigenmann, C. Ding, and S. A. McKee, Eds., ACM, pp. 171–183.

[38] LEUNG, A., GUPTA, M., AGARWAL, Y., GUPTA, R., JHALA, R., AND LERNER, S. Verifying GPU kernels by test amplification. In *ACM SIGPLAN Conference on Programming Language Design and Implementation, PLDI '12, Beijing, China - June 11 - 16, 2012* (2012), J. Vitek, H. Lin, and F. Tip, Eds., ACM, pp. 383–394.

[39] LI, G., AND GOPALAKRISHNAN, G. Scalable smt-based verification of GPU kernel functions. In *Proceedings of the 18th ACM SIGSOFT International Symposium on Foundations of Software Engineering, 2010, Santa Fe, NM, USA, November 7-11, 2010* (2010), G. Roman and A. van der Hoek, Eds., ACM, pp. 187–196.

[40] LI, G., LI, P., SAWAYA, G., GOPALAKRISHNAN, G., GHOSH, I., AND RAJAN, S. P. GKLEE: concolic verification and test generation for gpus. In *Proceedings of the 17th ACM SIGPLAN Symposium on Principles and Practice of Parallel Programming, PPOPP 2012, New Orleans, LA, USA, February 25-29, 2012* (2012), J. Ramanujam and P. Sadayappan, Eds., ACM, pp. 215–224.

[41] LITZKOW, M., TANNENBAUM, T., BASNEY, J., AND LIVNY, M. Checkpoint and migration of unix processes in the condor distributed processing system. Tech. rep., University of Wisconsin-Madison Department of Computer Sciences, 1997.

[42] MAI, H., ZHAO, J., ZHENG, H., ZHAO, Y., LIU, Z., GAO, M., WANG, C., CUI, H., FENG, X., AND KOZYRAKIS, C. Honeycomb: Secure and efficient GPU executions via static validation. In *17th USENIX Symposium on Operating Systems Design and Implementation (OSDI 23)* (Boston, MA, 2023), USENIX Association, pp. 155–172.

[43] META. Llama 2. <https://github.com/meta-llama/llama>, 2024.

[44] META. Llama 3.3. <https://huggingface.co/meta-llama/Llama-3.3-70B-Instruct>, 2024.

[45] MICROSOFT. What runs chatgpt inside microsoft’s ai supercomputer. <https://techcommunity.microsoft.com/blog/microsoftmechanicsblog/what-runs-chatgpt-inside-microsofts-ai-supercomputer--featuring-mark-russinovich/3830281>, 2025.

[46] MOHAN, J., PHANISHAYEE, A., AND CHIDAMBARAM, V. Checkfreq: Frequent, fine-grained DNN checkpointing. In *19th USENIX Conference on File and Storage Technologies, FAST 2021, February 23-25, 2021* (2021), M. K. Aguilera and G. Yadgar, Eds., USENIX Association, pp. 203–216.

[47] NVIDIA. Creating a communicator. <https://docs.nvidia.com/deeplearning/nccl/user-guide/docs/usage/communicators.html>, 2024.

[48] NVIDIA. Cuda toolkit 12.3 downloads. <https://developer.nvidia.com/cuda-12-3-0-download-archive>, 2024.

[49] NVIDIA. Cuda toolkit documentation - driver apis. <https://docs.nvidia.com/cuda/cuda-driver-api/index.html>, 2024.

[50] NVIDIA. Implement asynchronous checkpoint saving (with `-dist-ckpt-format torch_dist`). <https://github.com/NVIDIA/Megatron-LM/commit/cbb9c05c06b5fa32a8f5b47902751a7bc6d9f112>, 2024.

[51] NVIDIA. Parallel thread execution isa version 8.4. <https://docs.nvidia.com/cuda/parallel-thread-execution/index.html>, 2024.

[52] NVIDIA. Basic linear algebra on nvidia gpus. <https://developer.nvidia.com/cUBLAS>, 2025.

[53] NVIDIA. Context management. https://docs.nvidia.com/cuda/cuda-driver-api/group__CUDA__CTX.html, 2025.

[54] NVIDIA. Cuda binary utilities. <https://docs.nvidia.com/cuda/cuda-binary-utilities/index.html>, 2025.

[55] NVIDIA. Live migration for gpu-accelerated virtual machines. <https://www.nvidia.com/en-au/data-center/virtualization/virtual-gpu-migration/>, 2025.

[56] NVIDIA. Nvidia/cuda-checkpoint. <https://github.com/NVIDIA/cuda-checkpoint>, 2025.

[57] OPENAI. Openai gym. <https://github.com/openai/gym>, 2024.

[58] PYTORCH. Torchscript.

[59] PYTORCH. Cuda semantics. <https://pytorch.org/docs/stable/notes/cuda.html#cuda-memory-management>, 2024.

[60] PYTORCH. torchvision. <https://github.com/pytorch/vision>, 2024.

[61] SHAPIRO, J. S., SMITH, J. M., AND FARBER, D. J. EROS: a fast capability system. In *Proceedings of the 17th ACM Symposium on Operating System Principles, SOSP 1999, Kiawah Island Resort, near Charleston, South Carolina, USA, December 12-15, 1999* (1999), D. Kotz and J. Wilkes, Eds., ACM, pp. 170–185.

[62] SHAPIRO, J. S., SMITH, J. M., AND FARBER, D. J. EROS: a fast capability system. In *Proceedings of the 17th ACM Symposium on Operating System Principles, SOSP 1999, Kiawah Island Resort, near Charleston, South Carolina, USA, December 12-15, 1999* (1999), D. Kotz and J. Wilkes, Eds., ACM, pp. 170–185.

[63] SHUKLA, D., SIVATHANU, M., VISWANATHA, S., GULAVANI, B. S., NEHME, R., AGRAWAL, A., CHEN, C., KWATTRA, N., RAMJEE, R., SHARMA, P., KATIYAR, A., MODI, V., SHARMA, V., SINGH, A., SINGHAL, S., WELANKAR, K., XUN, L., ANUPINDI, R., ELANGOVAN, K., RAHMAN, H., LIN, Z., SEETHARAMAN, R., XU, C., AILIJIANG, E., KRISHNAPPA, S., AND RUSSINOVICH, M. Singularity: Planet-scale, preemptive and elastic scheduling of AI workloads. *CoRR abs/2202.07848* (2022).

[64] STOYANOV, R., SPISAKOVÁ, V., RAMOS, J., GURFINKEL, S., VAGIN, A., REBER, A., ARMOUR, W., AND BRUNO, R. Criugpu: Transparent checkpointing of gpu-accelerated workloads. *CoRR abs/2502.16631* (2025).

[65] STRATTON, J. A., RODRIGUES, C., SUNG, I.-J., OBEID, N., CHANG, L.-W., ANSSARI, N., LIU, G. D., AND HWU, W.-M. W. Parboil: A revised benchmark suite for scientific and commercial throughput computing. *Center for Reliable and High-Performance Computing* 127, 7.2 (2012).

[66] TSALAPATIS, E., HANCOCK, R., BARNES, T., AND MASHITZADEH, A. J. The aurora single level store operating system. In *Proceedings of the ACM SIGOPS 28th Symposium on Operating Systems Principles* (New York, NY, USA, 2021), SOSP ’21, Association for Computing Machinery, p. 788–803.

[67] USTIUGOV, D., PETROV, P., KOGIAS, M., BUGNION, E., AND GROT, B. Benchmarking, analysis, and optimization of serverless function snapshots. In *ASPLOS '21: 26th ACM International Conference on Architectural Support for Programming Languages and Operating Systems, Virtual Event, USA, April 19-23, 2021* (2021), T. Sherwood, E. D. Berger, and C. Kozyrakis, Eds., ACM, pp. 559–572.

[68] WAN, B., HAN, M., SHENG, Y., LAI, Z., ZHANG, M., ZHANG, J., PENG, Y., LIN, H., LIU, X., AND WU, C. Bytecheckpoint: A unified checkpointing system for LLM development. *CoRR abs/2407.20143* (2024).

[69] WANG, K. A., HO, R., AND WU, P. Replayable execution optimized for page sharing for a managed runtime environment. In *Proceedings of the Fourteenth EuroSys Conference 2019, Dresden, Germany, March 25-28, 2019* (2019), G. Cadea, R. van Renesse, and C. Fetzer, Eds., ACM, pp. 39:1–39:16.

[70] WANG, T., CHEN, Z., WEI, X., GU, J., CHEN, R., AND CHEN, H. Characterizing network requirements for GPU API remoting in AI applications. *CoRR abs/2401.13354* (2024).

[71] WANG, Z., JIA, Z., ZHENG, S., ZHANG, Z., FU, X., NG, T. S. E., AND WANG, Y. GEMINI: fast failure recovery in distributed training with in-memory checkpoints. In *Proceedings of the 29th Symposium on Operating Systems Principles, SOSP 2023, Koblenz, Germany, October 23-26, 2023* (2023), J. Flinn, M. I. Seltzer, P. Druschel, A. Kaufmann, and J. Mace, Eds., ACM, pp. 364–381.

[72] WEI, X., LU, F., WANG, T., GU, J., YANG, Y., CHEN, R., AND CHEN, H. No provisioned concurrency: Fast rdma-codedesigned remote fork for serverless computing. In *17th USENIX Symposium on Operating Systems Design and Implementation, OSDI 2023, Boston, MA, USA, July 10-12, 2023* (2023), R. Geambasu and E. Nightingale, Eds., USENIX Association, pp. 497–517.

[73] WU, F., DONG, M., MO, G., AND CHEN, H. Treesls: A whole-system persistent microkernel with tree-structured state checkpoint on NVM. In *Proceedings of the 29th Symposium on Operating Systems Principles, SOSP 2023, Koblenz, Germany, October 23-26, 2023* (2023), J. Flinn, M. I. Seltzer, P. Druschel, A. Kaufmann, and J. Mace, Eds., ACM, pp. 1–16.

[74] XIAO, W., BHARDWAJ, R., RAMJEE, R., SIVATHANU, M., KWATRA, N., HAN, Z., PATEL, P., PENG, X., ZHAO, H., ZHANG, Q., YANG, F., AND ZHOU, L. Gandiva: Introspective cluster scheduling for deep learning. In *13th USENIX Symposium on Operating Systems Design and Implementation, OSDI 2018, Carlsbad, CA, USA, October 8-10, 2018* (2018), A. C. Arpaci-Dusseau and G. Voelker, Eds., USENIX Association, pp. 595–610.

[75] YANG, Y., DU, D., SONG, H., AND XIA, Y. On-demand and parallel checkpoint/restore for gpu applications. In *Proceedings of the 2024 ACM Symposium on Cloud Computing (New York, NY, USA, 2024), SoCC '24*, Association for Computing Machinery, p. 415–433.

[76] YU, M., WANG, A., CHEN, D., YU, H., LUO, X., LI, Z., WANG, W., CHEN, R., NIE, D., AND YANG, H. Faaswap: Slo-aware, gpu-efficient serverless inference via model swapping. *CoRR abs/2306.03622* (2023).

[77] ZENG, S., XIE, M., GAO, S., CHEN, Y., AND LU, Y. Medusa: Accelerating serverless LLM inference with materialization. In *Proceedings of the 30th ACM International Conference on Architectural Support for Programming Languages and Operating Systems, Volume 1, ASPLOS 2025, Rotterdam, The Netherlands, 30 March 2025 - 3 April 2025* (2025), L. Eeckhout, G. Smaragdakis, K. Liang, A. Sampson, M. A. Kim, and C. J. Rossbach, Eds., ACM, pp. 653–668.

[78] ZHANG, S., ROLLER, S., GOYAL, N., ARTETXE, M., CHEN, M., CHEN, S., DEWAN, C., DIAB, M. T., LI, X., LIN, X. V., MIHAYLOV, T., OTT, M., SHLEIFER, S., SHUSTER, K., SIMIG, D., KOURA, P. S., SRIDHAR, A., WANG, T., AND ZETTLEMOYER, L. OPT: open pre-trained transformer language models. *CoRR abs/2205.01068* (2022).

Table 4: Detailed setups of applications evaluated in §8. * indicates a multi-GPU setup. PPO is training-only, and our setup cannot run Llama-3-70B training.

	ResNET-152M (R ^{152M})		PPO-336M (PPO ^{336M})		Stable Diffusion-1B (SD ^{1B})		Llama2-13B (L ^{13B})		Llama3.3-70B (L ^{70B})	
Application Library	Train	Inference	Train	Inference	Train*	Inference	Train*	Inference	Inference*	
	Torchvision [60]		OpenAI Gym [57]		HuggingFace [24]		Meta Llama 2 [43]		Meta Llama 3.3 [44]	
# GPU used	1	1	1	N/A	8	1	8	1	N/A	8
Total GPU Memory (per GPU)	1.8 GB	1.7 GB	5.9 GB	N/A	70.6 GB	8.9 GB	73.6 GB	55.4 GB	N/A	70.8 GB
# GPU buffers (per GPU)	209	195	75	N/A	445	234	413	347	N/A	718
# Active GPU kernels	13	8	41	N/A	51	50	36	74	N/A	73

```

import phos
+ optimal_frequency = phos.calculate_optimal_frequency(...)
+ cur_ckpt = 0

for batch_idx, batch in enumerate(dataloader):
    inputs = {k: v.to(device) for k, v in batch.items()}

    # checkpoint at the beginning of the iteration
+    if cur_ckpt % optimal_frequency == 0:
        ## This is an asynchronous call!
+        phos.checkpoint(ckpt_name, pid, mode='cow', ...)
+    cur_ckpt += 1

    outputs = model(**inputs)
    loss = outputs.loss
    loss.backward()

    torch.cuda.synchronize()
    optimizer.step() # update the most buffers
    optimizer.zero_grad()

```

Figure 21: An illustration of how applications can use PHOS SDK to control the checkpoint timing. Lines with + are code interacting with PHOS.

A Appendix

A.1 Determine the optimal checkpoint frequency

Problem formulation. Suppose we have N GPUs involved in a distributed computing job, and each GPU fails F times within an hour. Suppose each GPU failure is independent and identically distributed (i.i.d.), following a uniform distribution over the entire computation interval (T). The checkpoint overhead is O with PHOS. If a GPU fails, PHOS will stop all the GPU processes, and restore from the latest checkpoint. The restore time is R for all the GPUs.

The total GPU hour wasted due to failure is at a checkpoint frequency f times per hour:

$$(NFT) \times \left(R + \frac{N}{2f}\right).$$

The total GPU hours wasted due to checkpoint overhead is:

$$NOfT.$$

Put it all together: to total GPU hours wasted due to checkpoint overhead and failure recovery is:

$$\text{Total GPU-hours wasted} = NFT \left(R + \frac{N}{2f} \right) + NOfT.$$

Solving the optimal f . For a given job, the distribution of failures (F), the checkpoint overhead (O), and the restore time (R) are static and can be profiled online [46], so we only need to solve the checkpoint frequency f to minimize the total GPU hours wasted. By differentiating the total GPU hours wasted with respect to f , we got:

$$f^* = \sqrt{\frac{NF}{2O}}.$$

PHOS sets the checkpoint frequency to f^* for each computing job.

A.2 PHOS software development kit (SDK)

Applications can explicitly call our SDK to control the timing of checkpointing and the protocol used, see Figure 21. Thanks to our OS-level design, the code change is minimal: it only needs one line of code. In our example, the code tells PHOS that it needs to checkpoint the process at the beginning of an iteration of a training GPU process. Note that the `checkpoint` is asynchronously called so it will not block application execution unless the last checkpoint is not done.

A.3 Detailed setups of our evaluated applications

Table 4 shows the detailed buffer allocation information as well as the number of GPU kernels information of our evaluated applications. The detailed setups of training workloads are as follows: For ResNet50 training, we use the CIFAR-10 dataset and configure a batch size of 32 for training. For PPO training, we use the gym code [57]. For Stable Diffusion training, we use the SD v1-4 model and a batch size of 1,536 for each GPU. Finally, for Llama training, we use a distributed configuration of 8TP, the batch size is 4, restricted by the available GPU memory. All the training workloads use the AdamW optimizer.